Systematic study of dynamical dipole mode via the isospin-dependent Boltzmann-Uehling-Uhlenbeck model[*]

YE Shao-Qiang (叶绍强),[1,2] CAI Xiang-Zhou (蔡翔舟),[1] FANG De-Qing (方德清),[1]
MA Yu-Gang (马余刚),[1,†] and SHEN Wen-Qing (沈文庆)[1]

[1]*Shanghai Institute of Applied Physics, Chinese Academy of Sciences, Shanghai 201800, China*
[2]*University of Chinese Academy of Sciences, Beijing 100039, China*

Dynamical dipole mode in heavy-ion collisions has been studied by using an isospin-dependent Boltzmann-Uehling-Uhlenbeck (IBUU) model. We investigate the dependence of centroid energy and strength of the γ spectrum on beam energy, N/Z ratio and mass asymmetry. The calculated yield and angular distribution of the γ-ray produced by dynamical dipole emission are consistent with the experimental data. The results show that the detailed study of dynamical dipole radiation can provide information on the isospin evolution of charge-asymmetric heavy-ion collisions around the normal nuclear density.

I. INTRODUCTION

The giant dipole resonance (GDR), a collective mode of the nucleons, which plays an important role in nuclear physics research, has been widely studied experimentally [1–3] and theoretically [4, 5] during the past decades. The pre-equilibrium GDR (dynamical dipole mode), generated by a collective motion of protons against neutrons before the formation of a fully equilibrated compound nucleus (CN), has become a hot topic [6–17]. During the early stage of charge-asymmetric heavy-ion collisions, a large amplitude collective dipole oscillation is triggered along the symmetry axis of the strongly deformed composite system; the oscillation emits prompt photons, called dynamical dipole radiation, in addition to the photons originating from a thermal excited GDR of the hot CN. The γ yield from the pre-equilibrium GDR contains lots of information about the early stage of collisions when the CN is still in a highly deformed configuration.

Several microscopic transport models, such as time-dependent Hartree-Fock (TDHF) [15], Boltzmann-Nordheim-Vlasov (BNV) [17], constrained molecular dynamics (CoMD) [16], and isospin-dependent quantum molecular dynamics (IQMD) [18–20], have been successfully applied to study properties of the dynamical dipole emission. A "bremsstrahlung" approach derived in Refs. [13, 14] was widely adopted to estimate the contribution of this pre-equilibrium collective dipole radiation emission. Here we use the isospin-dependent Boltzmann-Uehling-Uhlenbeck (IBUU) transport model [21] to make systematical calculations of the γ yield and the emission anisotropy of such prompt dipole radiation.

II. DESCRIPTION OF THE METHOD

The IBUU model [22] is widely used for treating heavy-ion collision dynamics and extracting important information of nuclear matter. The BUU equation reads

$$
\begin{aligned}
\frac{\partial f}{\partial t} &+ v \cdot \nabla_r f - \nabla_r U \cdot \nabla_p f \\
&= \frac{4}{(2\pi)^3} \int \mathrm{d}^3 p_2 \mathrm{d}^3 p_3 \mathrm{d}\Omega \frac{\mathrm{d}\sigma_{NN}}{\mathrm{d}\Omega} V_{12} \\
&\times [f_3 f_4 (1-f)(1-f_2) - f f_2 (1-f_3)(1-f_4)] \\
&\times \delta^3 (p + p_2 - p_3 - p_4),
\end{aligned}
\tag{1}
$$

where $\mathrm{d}\sigma_{NN}/\mathrm{d}\Omega$ is in-medium nucleon-nucleon cross section, V_{12} is relative velocity for the colliding nucleons. U is the mean field potential which includes the isospin-dependent term, f is the single particle distribution function, and p is the corresponding momentum. The isospin dependence is incorporated into the model through the initialization and nuclear mean field. The mean field including isospin symmetry term is parameterized as

$$
U(\rho, \tau_z) = a\left(\frac{\rho}{\rho_0}\right) + b\left(\frac{\rho}{\rho_0}\right)^\sigma + V_{\mathrm{asy}}^{n(p)}(\rho, \delta),
\tag{2}
$$

where ρ_0 is the saturation nuclear matter density, and $\rho = \rho_n + \rho_p$ is density of nucleon; ρ_n and ρ_p are the neutron and proton densities, respectively. The coefficients a, b and σ are parameters for the equation of state (EOS). Here we choose the parameters corresponding to the soft EOS with the compressibility K of $200\,\mathrm{MeV}$ ($a = -356\,\mathrm{MeV}$, $b = 303\,\mathrm{MeV}$, and $\sigma = 7/6$). The form of single particle symmetry potential [23–25] reads

$$
\begin{aligned}
V_{\mathrm{asy}}^{n(p)}(\rho, \delta) &= \frac{\partial}{\partial \rho}\left[\frac{C_{s,p}}{2}\left(\frac{\rho}{\rho_0}\right)^\gamma \rho \delta^2\right] \\
&= \frac{C_{s,p}}{2}\left[(\gamma - 1)\left(\frac{\rho}{\rho_0}\right)^\gamma \delta^2 \pm 2\left(\frac{\rho}{\rho_0}\right)^\gamma \delta\right],
\end{aligned}
\tag{3}
$$

where $C_{s,p}$ is the symmetry energy coefficient depending on the different densities of neutrons and protons in nuclear medium. In this paper, we use the measured symmetry energy of $C_{s,p} = 35.19$ MeV and, also, a soft symmetry energy ($\gamma = 0.5$), which was found to describe the experiment data reasonably well in Ref. [17, 26]. As usual, the test particle method is applied in the IBUU simulations and the in-medium nucleon-nucleon cross section is taken into account [27]. For calculating dynamic dipole emission, the emitted nucleons with their local density below $\rho_0/8$ are excluded.

During pre-equilibrium dipole oscillation, a larger initial dipole moment triggers higher amplitude isovector oscillations, which increases the chance of a clear experimental observation. The giant dipole moment in coordinator space $D(t)$ is defined as [14]

$$D(t) = \frac{NZ}{A}X(t) = \frac{NZ}{A}(R_p - R_n), \qquad (4)$$

where $A = N + Z$, $N = N_p + N_t$, $Z = Z_p + Z_t$ are the total number of participating nucleons, neutrons, and protons from the projectile (p) and the target (t), respectively; $X(t)$ is the distance between the centers of protons and neutrons; and R_p and R_n are the total coordinates of center-of-mass system for the protons and neutrons, respectively. And the canonical conjugate momentum of $D(t)$ is written as

$$DK(t) = \frac{NZ}{A}(\frac{P_p}{Z} - \frac{P_n}{N}), \qquad (5)$$

where P_p and P_n are the total momenta of center-of-mass system for the protons and neutrons, respectively. The initial ($t = 0$: touching configuration) giant dipole moment can be expressed as

$$D(t = 0) = \frac{NZ}{A}X(t = 0) = \frac{R_p + R_t}{N + Z}Z_pZ_t(\frac{N_p}{Z_p} - \frac{N_t}{Z_t}), \qquad (6)$$

where R_p and R_t are the radii of the projectile and target, respectively [13].

Then, as given by the bremsstrahlung approach, the γ yield can be extracted as [13, 14]

$$\frac{\mathrm{d}P}{\mathrm{d}E_\gamma} = \frac{2e^2}{3\pi\hbar c^3 E_\gamma} \mid D''(\omega) \mid^2, \qquad (7)$$

where $E_\gamma = \hbar\omega$ is photon energy and $\mid D''(\omega) \mid^2$ is the Fourier transform of the dipole "acceleration" $D''(\omega) = \int_{t_0}^{t_{\max}} D''(t)e^{i\omega t}\mathrm{d}t$. For each event, t_0 represents the onset-time of the collective dipole response (phase-space spiraling) and $t_{\max}$ is the "damping time".

Recently, a clear anisotropy for the angular distribution of the total γ spectrum has been observed [10, 11]. For the dipole oscillation just along the beam axis, the angular distribution is expected to be given by the Legendre polynomial expansion $M(\theta) \sim \sin^2\theta \sim 1 + a_2P_2(\cos\theta)$ (a_2 is the anisotropy parameter and θ is the polar angle between the photon-emitting direction and oscillation axis). For the dynamical dipole mode, the prompt dipole axis rotates during the emission.

First, in a very small time interval Δt, φ_i and φ_f are defined as the initial and final angles of the oscillation axis with respect to the beam axis, respectively. So $\Delta\varphi = \varphi_f - \varphi_i$ is the rotation angle during the time interval Δt. From preceding text, the angular distribution in Δt can be averaged over the angle $\Delta\varphi$ as $M(\theta) \sim 1 - (1/4 + 3x/4)P_2(\cos\theta)$, where $x = \cos(\varphi_f + \varphi_i)\sin(\varphi_f - \varphi_i)/(\varphi_f - \varphi_i)$ [17]. Then, for the whole time of the dynamical dipole, we can extract the angular distribution by using a weighted form for every time step and summing over all of them: $M(\theta) = \sum_{i=1}^{t_{\max}} \beta_i M(\theta, \Phi_i)$, where Φ_i is the rotation angle and β_i is the radiation emission probability. From Eq. (7) we have $\beta_i = P(t_i) - P(t_{i-1})$ where $P(t_i) = \int_{t_0}^{t_i} \mid D''(t) \mid^2 \mathrm{d}t/P_{\mathrm{tot}}$, and P_{tot} is given by $P(t_{\max})$, which is the total emission probability at the final dynamical dipole damped time. Finally, the anisotropy parameter is:

$$a_2 = \sum_{i=1}^{t_{\max}} \beta_i(\frac{1}{4} + \frac{3}{4}x). \qquad (8)$$

The angular distribution of the prompt γ emission has been extracted by using the formalism from Ref.[17].
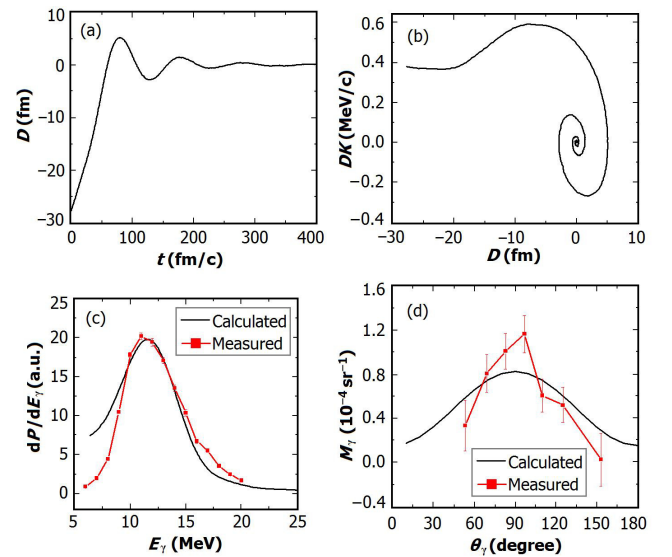
III. RESULTS AND DISCUSSION

Fig. 1. (Color online) The results in 16 MeV/nucleon ^{36}Ar + ^{96}Zr with $b = 4$ fm: time evolution of dipole moment $D(t)$ in coordinate space (a), dipole phase-space correlation (b), and comparison of the γ yield (c) and angular distribution (d) between our calculations and experimental data under the same conditions.

Figures 1(a) and 1(b) show the time evolution of the dipole moment $D(t)$ and the phase space correlation (spiraling) between $D(t)$ and $DK(t)$ for the 16 MeV/nucleon ^{36}Ar + ^{96}Zr with $b = 4$ fm. One sees that the large amplitude of the first oscillation decaying rapidly within several periods,
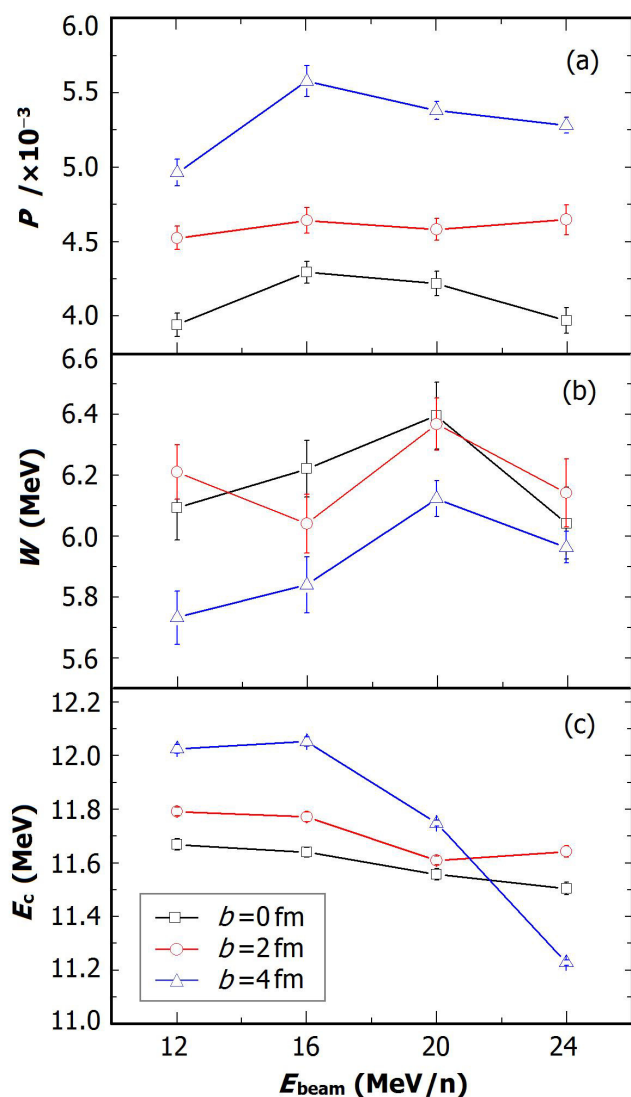
Fig. 2. (Color online) Evolution of (a) the total strength (P), (b) the width (W) and (c) the central energy (E_c) of γ spectrum in the ^{36}Ar + ^{96}Zr reactions at $E_{\text{beam}} = 12$, 16, 20 and 24 MeV/nucleon with $b = 0$, 2 and 4 fm.

Fig. 3. (Color online) Anisotropy parameter of ^{36}Ar + ^{96}Zr at different incident energies and impact parameters.

have shown that γ spectrum of the dynamical dipole mode is dependent on beam energy of the reaction system. In this paper, detailed results are drawn from the dynamical emission of 12, 16, 20 and 24 MeV/nucleon ^{36}Ar + ^{96}Zr with different impact parameters. Using the Lorentz fitting, we extract the central energy (E_c), the width (W), and the total strength (P) of the γ spectrum (Fig. 2).

As shown in Fig. 2(a), the strength has a maximum value around $E_{\text{beam}} = 16$ MeV/nucleon, which is the same as the results in Ref. [14]. At low incident energies, the dipole oscillation increases fiercely with E_{beam}; while at high incident energies, the damping properties of the dipole moment become stronger and fast nucleon emission takes place which make the dipole oscillation become weaker [26]. The damping properties and the nucleon emission also lead to the evolutionary trend of dynamical dipole emission width (Fig. 2(b)). In Fig. 2(c), the dynamical vibration has a high frequency at low incident energies. This means a faster isospin equilibration in the collisions at lower beam energies, which was concluded similarly in Ref. [28]. Also, the strength of γ radiation increases obviously with the impact parameter, because of the increasing dipole moment on the direction perpendicular to the beam. The central energy of γ spectrum has the same behavior, because part of the beam energy transfers to the rotational energy of CN when the reaction happens away from the central collision.

Figure 3 shows the calculation results of anisotropy parameters (a_2) of ^{36}Ar + ^{96}Zr at different incident energies and impact parameters. The a_2 value decreases faster at higher incident energies, because higher beam energy causes faster rotation of the oscillation axis. The same thing happens as the impact parameter becomes larger.

The dynamical dipole emission originates from different N/Z ratios ($R_{N/Z}$) between target and projectile, which leads to the process of charge equilibration. Fig. 4 shows the E_c and P of the γ spectrum produced by reaction systems of ^{36}Ar + ^{96}Zr ($R_{N/Z} = 1.400$), ^{36}Ar + ^{96}Mo ($R_{N/Z} = 1.286$) and

and the whole process continues for about 300 fm/c. Especially, Fig. 1(b) shows the collective oscillation initiated at the very early time, which corresponds to the touching configuration value of the collision. So, in this paper, we define $t_{\text{max}} - t_0 = 300$ fm/c to make sure that the collective oscillation is basically over. In Fig. 1(c), the calculated photon yields for the 16 MeV/nucleon ^{36}Ar + ^{96}Zr are compared with the experimental data [10]. Fig. 1(d) shows the angular distribution, both the simulation and experimental results are averaged from data obtained at impact parameters of $b = 0$, 2 and 4 fm. Our calculation results can reproduce the experimental data fairly well, indicating that the model is successful in describing the γ radiation of dynamical dipole mode.

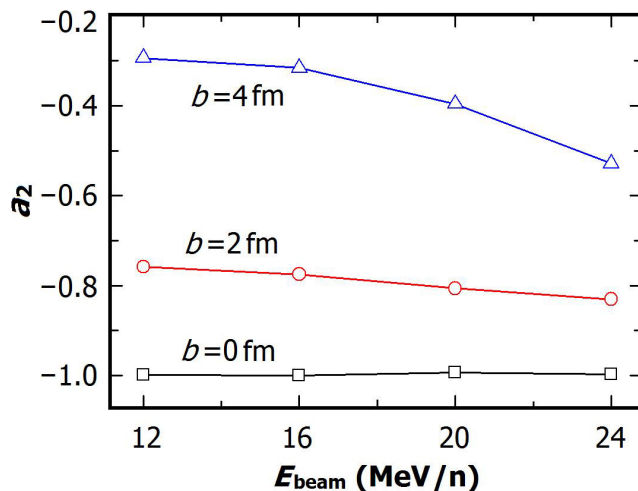So far, both experimental data and theoretical calculations

ChinaXiv

YE Shao-Qiang *et al.*   Nucl. Sci. Tech. **25**, 030501 (2014)
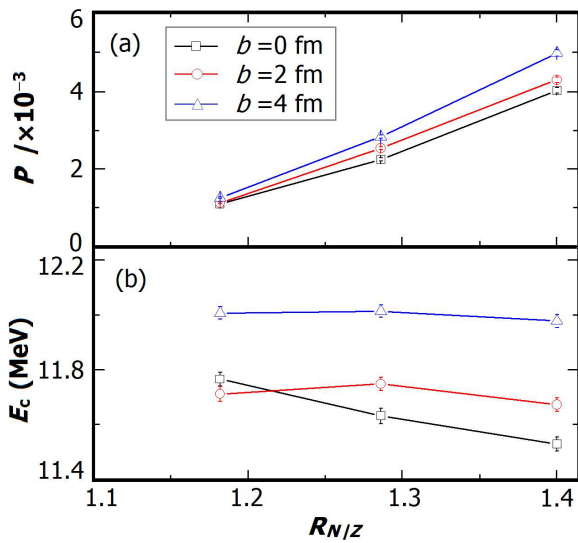
Fig. 4. (Color online) Calculated (a) total strength (P) and (b) central energy (E_c) of the γ spectrum produced by the reactions of ^{36}Ar + ^{96}Zr ($R_{N/Z} = 1.400$), ^{36}Ar+^{96}Mo ($R_{N/Z} = 1.286$) and ^{36}Ar+^{96}Ru ($R_{N/Z} = 1.182$) at 16 MeV/nucleon with different impact parameters.
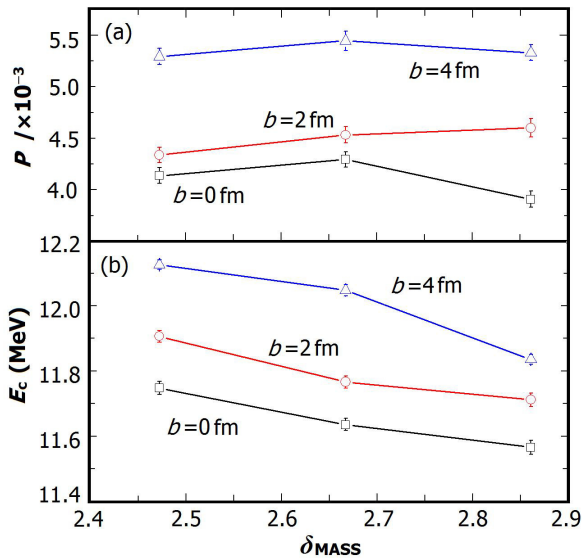

Fig. 5. (Color online) Calculated (a) total strength (P) and (b) central energy (E_c) of the γ spectrum produced by the reactions of ^{36}Ar + ^{89}Rb ($\delta_{\text{MASS}} = 2.472$), ^{36}Ar + ^{96}Zr ($\delta_{\text{MASS}} = 2.667$) and ^{36}Ar + ^{103}Tc ($\delta_{\text{MASS}} = 2.861$) at 16 MeV/nucleon with different impact parameters.

^{36}Ar + ^{96}Ru ($R_{N/Z} = 1.182$) at 16 MeV/nucleon. Fig. 4(a) demonstrates a sharp monotonic increasing behavior in the correlation between $R_{N/Z}$ and P. The large difference of dipole moments at the incident channel is responsible for this behavior. In Fig. 4(b), the E_c varies just a little at different values of $R_{N/Z}$, but increases with the impact parameters. Besides, at each impact parameter, the anisotropy parameters (a_2) of different reactions are almost the same (not shown).

To study the influence of mass asymmetry, the reactions of ^{36}Ar + ^{89}Rb, ^{36}Ar + ^{96}Zr and ^{36}Ar + ^{103}Tc at 16 MeV/nucleon are calculated. The N/Z ratios of these systems are the same ($R_{N/Z} = 1.400$), but the parameters of mass asymmetry ($\delta_{\text{MASS}} = \text{MASS}_{\text{target}}/\text{MASS}_{\text{projectile}}$) are 2.472, 2.667 and 2.861, respectively. Compared with the results in Fig. 4, an opposite behavior is seen in Fig. 5: the variation of P is small and the E_c has a decreasing tendency with a larger δ_{MASS}. But all of them increase monotonously with the impact parameter. The yields of dynamical dipole radiation are mainly dependent on incident energy and the N/Z ratio. And the results of anisotropy parameters at different values of δ_{MASS} are similar to the case of charge asymmetry. In other words, the major effects on the angular distribution are the beam energy and the impact parameter.

IV. SUMMARY

In this paper, we use the IBUU model to study the properties of the dynamical dipole mode via a collective bremsstrahlung mechanism in fusion reactions with charge-asymmetric systems. We compare the γ spectrum and angular distribution of the prompt photon radiation with the experimental data, and show the features of this dynamical dipole emission with low energy reactions of different systems. We study the total emission probability, centroid energy and angular distribution of the pre-equilibrium dipole oscillation and their dependence on incident energy, N/Z ratio and mass asymmetry. Our results demonstrate that the total emission probability of the dynamical dipole mode has a strong dependence on beam energy and charge asymmetry in the entrance channel, besides on mass asymmetry. The central energy of this pre-equilibrium dipole oscillation is more sensitive to the beam energy and mass asymmetry than the case of charge asymmetry. And just the beam energy has an influence on the anisotropy of the prompt photon radiation. But, almost, all of the features are sensitive to the impact parameters. So, this work indicates that detailed study of dynamical dipole radiation can be used as a probe to extract information on the early stage of charge-asymmetric heavy-ion collisions around the normal nuclear density.

[1] Snover K A. Annu Rev Nucl Part Sci, 1986, **36**: 545–606.
[2] Gaardhoje J J. Annu Rev Nucl Part Sci, 1992, **42**: 483–536.
[3] Papa M, Bonanno A, Amorini F, *et al*. Phys Rev C, 2003, **68**: 034606.
[4] Hofmann H, Gregoire C, Lucas R, *et al*. Z Phys A, 1979, **293**: 229–240.
[5] Ditoro M and Gregoire C. Z Phys A, 1985, **320**: 321–325.
[6] Santonocito D and Blumenfeld Y. Eur Phys J A, 2006, **30**: 183–202.
[7] Flibotte S, Chomaz P, Colonna M, *et al*. Phys Rev Lett, 1996,

ChinaXiv

SYSTEMATIC STUDY OF DYNAMICAL . . .   Nucl. Sci. Tech. **25**, 030501 (2014)

77: 1448–1451.

[8] Pierroutsakou D, Di Toro M, Amorini F, *et al*. Eur Phys J A, 2003, **16**: 423–435.

[9] Pierroutsakou D, Martin B, Inglima G, *et al*. Phys Rev C, 2005, **71**: 054605.

[10] Pierroutsakou D, Martin B, Agodi C, *et al*. Phys Rev C, 2009, **80**: 024612.

[11] Martin B, Pierroutsakou D, Agodi C, *et al*. Phys Lett B, 2008, **664**, 47–51.

[12] Chomaz P, Ditoro M, Smerzi A. Nucl Phys A, 1993, **563**: 509–524.

[13] Baran V, Cabibbo M, Colonna M, *et al*. Nucl Phys A, 2001, **679**: 373–392.

[14] Baran V, Brink D M, Colonna M, *et al*. Phys Rev Lett, 2001, **87**: 182501.

[15] Simenel C, Chomaz P, de France G. Phys Rev C, 2007, **76**: 024609.

[16] Papa M, Tian W D, Giuliani G, *et al*. Phys Rev C, 2005, **72**: 064608.

[17] Baran V, Rizzo C, Colonna M, *et al*. Phys Rev C, 2009, **79**: 021603.

[18] Wu H L, Tian W D, Ma Y G, *et al*. Phys. Rev. C, 2010, **81**: 047602.

[19] Tao C, Ma Y G, Zhang G Q, *et al*. Phys Rev C, 2013, **87**: 014621.

[20] Tao C, Ma Y G, Zhang G Q, *et al*. Nucl Sci Tech, 2013, **24**: 030502.

[21] Ma Y G, Liu G H, Cai X Z, *et al*. Phys Rev C, 2012, **85**: 024618.

[22] Bauer W, Bertsch G F, Cassing W, *et al*. Phys Rev C, 1986, **34**, 2127–2133.

[23] Zhang Y X, Li Z X, Zhao K, *et al*. Nucl Sci Tech, 2013, **24**: 050503.

[24] Jiang W Z. Nucl Sci Tech, 2013, **24**: 050507.

[25] Kumar S and Ma Y G. Nucl Sci Tech, 2013, **24**: 050509.

[26] Ye S Q, Cai X Z, Ma Y G, *et al*. Phys Rev C, 2013, **88**: 047602.

[27] Li G Q and Machleidt R. Phys Rev C, 1993, **48**: 1702–1712; Phys Rev C, 1994, **49**: 566–569.

[28] Iwata Y, Otsuka T, Maruhn J A, *et al*. Phys Rev Lett, 2010, **104**: 252501.

chinaXiv:202306.00483v1